Original Article

Characteristics of the immune microenvironment and their clinical significance in lung adenocarcinoma patients with different ALK fusion variants

Yinbo Xiao, Hao Wang, Junliang Lu, Junyi Pang, Shiyi Liu, Yang Zhou, Xiaohua Shi*, Zhiyong Liang*

Department of Pathology, Molecular Pathology Research Center, Peking Union Medical College Hospital, Chinese Academy of Medical Science and Peking Union Medical College, Beijing, China

Contributions: (I) Conception and design: Y Xiao, X Shi, Z Liang; (II) Administrative support: X Shi, Z Liang; (III) Provision of study materials or patients: X Shi, Z Liang; (IV) Collection and assembly of data: Y Xiao, H Wang, Y Zhou; (V) Data analysis and interpretation: Y Xiao, H Wang, J Lu, J Pang, S Liu; (VI) Manuscript writing: All authors; (VII) Final approval of manuscript: All authors.

*These authors contributed equally to this work.

Correspondence to: Xiaohua Shi, MD, PhD; Zhiyong Liang, MD, PhD. Department of Pathology, State Key Laboratory of Complex Severe and Rare Diseases, Molecular Pathology Research Center, Peking Union Medical College Hospital, Chinese Academy of Medical Science and Peking Union Medical College, No. 1 Shuaifuyuan, Dongcheng District, Beijing 100730, China. Email: shixiaohua3762@foxmail.com; liangzy@pumch.cn.

Background: The tumor immune microenvironment of anaplastic lymphoma kinase (ALK)-rearranged lung adenocarcinoma (LUAD) stratified by ALK fusion variants is poorly pictured. Hence, in this study, we aim to explore the immune heterogeneity of ALK$^+$ LUAD across different ALK fusion variants and further investigate their significance on clinical prognosis.

Methods: A retrospective analysis was conducted on ALK$^+$ LUAD patients (N=68). DNA and RNA-based next-generation sequencing (NGS) was performed to clarify the specific ALK fusion variants. Clinical and pathological characteristics were compared between long and short ALK variants. To research the immune heterogeneity, multi-fluorescence was carried out to explore the differences in immune properties, such as tumor-infiltrating lymphocyte (TIL) number, TIL subset, and tertiary lymphoid structures (TLS) development, between long and short ALK variants. Furthermore, the prognostic value of these characteristics was analyzed. Finally, the expression of lymphocyte-activation gene-3 (LAG3), one novel immune therapy target, was assessed across ALK$^+$ LUAD.

Results: LUAD patients with short ALK fusion variant-driven tumors exhibited higher American Joint Committee on Cancer (AJCC) stage as well as larger tumor size than those with long ALK fusion variant-driven tumors. Compared to long ALK fusion variants, there were more TILs, especially natural killer (NK) cells, within short ALK variants. However, fewer TLS were established in cancers harboring short ALK variants than those with long ALK variants. In advanced-stage LUAD patients with ALK fusion, short ALK variants, hot immune status, and high-level NK cells were identified to be adverse prognostic factors, while high-level B cells, as well as the development of TLS, served as positive prognostic factors. As for LAG3 expression, LAG3$^+$ immune cells were more enriched in short ALK variants than in long ALK variants.

Conclusions: LUAD patients with short ALK fusion variant-driven tumors exhibited worse prognosis than those with long ALK fusion variant-driven tumors. The tumor immune microenvironments are heterogeneous across different ALK fusion variants with short variants characterized by higher levels of TIL, especially NK cells, but by less TLS development than long variants ALK$^+$ LUAD, which disfavor disease outcomes.

Keywords: Anaplastic lymphoma kinase (ALK); lung adenocarcinoma (LUAD); tumor microenvironment (TME); immunotherapy

Submitted Aug 04, 2024. Accepted for publication Dec 11, 2024. Published online Dec 27, 2024.
doi: 10.21037/tlcr-24-682
View this article at: https://dx.doi.org/10.21037/tlcr-24-682

Introduction

Oncogenic anaplastic lymphoma kinase (ALK) rearrangement defines a specific molecular subset of lung adenocarcinoma (LUAD), called ALK$^+$ LUAD (1). These cancers are characterized by being initially sensitive and beneficial from tyrosine kinase inhibitors (TKIs) therapy. To date, five TKIs have been approved by the US Food and Drug Administration (FDA) for ALK$^+$ LUAD treatment, including crizotinib (2), alectinib (3), ceritinib (4), brigatinib (5), and lorlatinib (2). Such targeted therapy has consistently shown superior efficacy and significantly improved the prognosis of ALK$^+$ LUAD patients. However, clinical response varies across patients, and further, nearly all patients inevitably develop resistance to TKIs (6), which remains a clinical challenge.

Accumulating evidence has demonstrated that the response to TKI treatment is potentially associated with the ALK fusion variant heterogeneity (7). Echinoderm microtubule-associated protein-like 4 (EML4) is identified to be the predominant fusion partner in LUAD cases with ALK rearrangements, accounting for 90% of all patients with ALK fusion (8,9). EML4-ALK fusion can be further classified into two subsets, including long variants which encode the full-length of EML4 protein (e.g., V1 and V2), and short variants which lack tandem atypical β-propeller (TAPE) domain of EML4 protein (e.g., V3 and V5) (10). *In-vitro* work has revealed that V3-carrying cells exhibited increased ALK phosphorylation and a higher half maximal inhibitory concentration (IC_{50}) to various TKIs than V1-carrying or V2-carrying cells (11). In the clinic, it is emerging that patients harboring short EML4-ALK variants exhibit worse progression-free survival (PFS) to TKI treatment as well as more aggressive behaviors compared with patients with other long ALK fusion variants (11-14). Thus, to overcome TKI resistance caused by ALK fusion variants and improve the overall prognosis, developing other novel therapies as an alternative strategy provides enhanced prospects for ALK$^+$ LUAD treatment.

Currently, immune therapy, such as programmed cell death protein 1 (PD-1)/programmed cell death ligand 1 (PD-L1) therapy, is a promising option for the treatment of advanced lung cancer without oncogene mutations (15). However, regarding ALK-fusion lung cancer, the relative inefficacy of PD-1/PD-L1 therapy has been reported in real-world clinical trials (16-18). These data suggest that other immune-modulating approaches beyond the PD-1/PD-L1 axis may better support ALK$^+$ tumor clearance. Several clinical trials are ongoing to test the efficacy of other novel immunotherapy, such as tumor-infiltrating lymphocytes (TILs) therapy and adoptive cell autologous natural killer (NK) cell therapy, for the treatment of ALK$^+$ LUAD patients. Moreover, recent work has demonstrated that the immune properties, such as immune cell function (19) and PD-L1 expression (20), vary among

Highlight box

Key findings

- Compared to long anaplastic lymphoma kinase (ALK) fusion variants, there were more tumor-infiltrating lymphocytes (TILs), especially natural killer (NK) cells, within short ALK variants. However, fewer tertiary lymphoid structures (TLSs) were established within short ALK variants than in long ALK variants.
- Short ALK variants, hot immune status, and high-level NK cells were identified to be negative prognostic factors for clinical outcomes in lung adenocarcinoma (LUAD) patients with ALK fusion, while high-level B cells and TLS development were identified to be positive prognostic factors for clinical outcomes in LUAD patients with ALK fusion.
- Lymphocyte-activation gene-3 (LAG3) positive immune cells were more enriched in short ALK variants than in long ALK variants.

What is known and what is new?

- The ALK fusion variant heterogeneity is potentially associated with the clinical prognosis of ALK$^+$ LUAD, as well as their response to tyrosine kinase inhibitor (TKI) treatment. In recent years, several studies have demonstrated that LUAD with different ALK fusion variants do impact the local immune microenvironment. However, to date, there is no study to characterize the immune microenvironment of LUAD among different ALK fusion variants.

What is the implication, and what should change now?

- Distinct immune properties of ALK$^+$ LUAD with short variants from those with long variants could determine their worse clinical prognosis. Immunotherapy for ALK-rearranged patients with short ALK fusion variants could be beneficial for immunotherapy beyond programmed cell death protein 1 (PD-1)/programmed cell death ligand 1 (PD-L1) therapy, such as anti-LAG3 therapy, which provides the theoretical foundation to explore novel immune therapies for ALK+ LUAD.

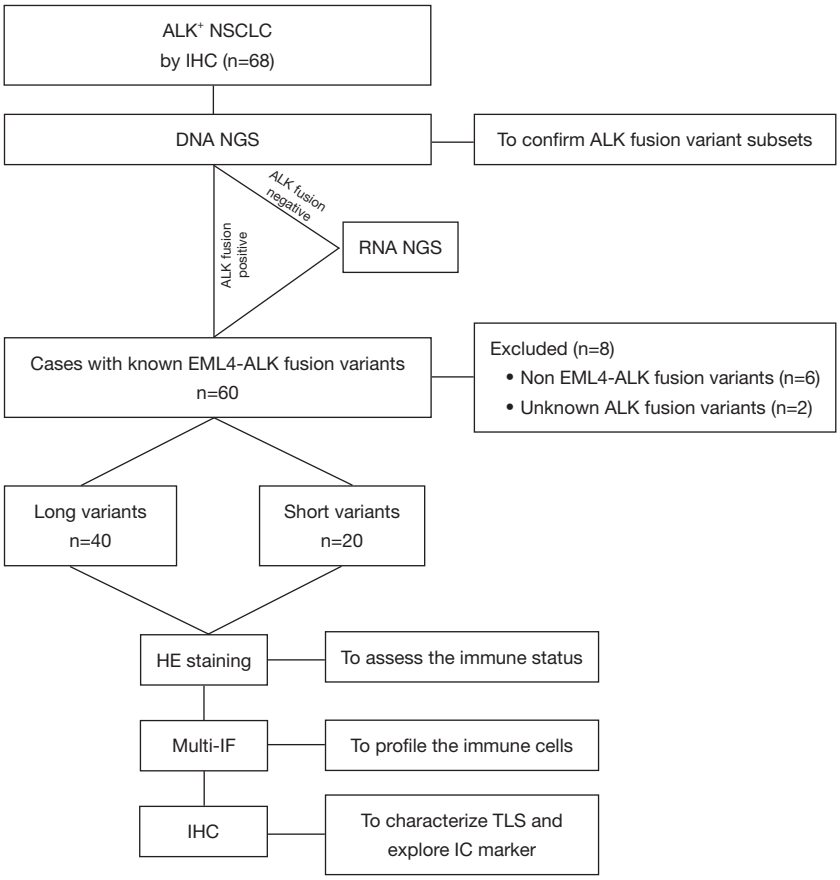

Figure 1 Flowchart of the study design for patient selection. ALK, anaplastic lymphoma kinase; NSCLC, non-small cell lung cancer; IHC, immunohistochemistry; NGS, next-generation sequencing; EML4, echinoderm microtubule-associated protein-like 4; HE, hematoxylin-eosin; multi-IF, multi-fluorescence; IC, immune cell; TLS, tertiary lymphoid structure.

patients with different ALK fusion variants. The heterogeneity of immune properties highlights that the selection of immune therapy should be determined with consideration of the ALK fusion variants. Thus, it is critical to clarify the immune microenvironment among different ALK fusion variants, but the details remain unclear.

Herein, in this study, we comprehensively investigated the immune microenvironment among LUAD with different ALK fusion variants and further explored the impacts of these characteristics on the clinical outcomes. Initially, the clinical and pathological characteristics of different ALK fusion variants were summarized. Subsequently, immune microenvironment properties across different ALK fusion variants were explored by histological quantification and multi-fluorescence (multi-IF) staining. The TIL number, TIL subsets, and TIL structure [e.g., tertiary lymphoid structures (TLSs)] were compared between the long-variant group and the short-variant group. Afterwards, the impacts of the ALK fusion variants as well as the immune status on the outcome of ALK$^+$ LUAD patients were further investigated. Finally, lymphocyte-activation gene-3 (LAG3), one novel immune therapy target, was evaluated across patients with different ALK fusion variants, which provides the theoretical foundation for ALK$^+$ LUAD immune therapy. We present this article in accordance with the REMARK reporting checklist (available at https://tlcr.amegroups.com/article/view/10.21037/tlcr-24-682/rc).

Methods

Cases

The flow chart is illustrated in *Figure 1*. From February 2019 to July 2022 in Peking Union Medical College

Hospital, we screened 68 LUAD patients with positive ALK immunohistochemistry (IHC). Experienced pathologists performed the histological diagnosis on formalin-fixed and paraffin-embedded tissue according to the World Health Organization (WHO) criteria (21,22). The histological patterns of LUAD were classified as Lepidic, Acinar, Papillary, High grade (such as solid and micropapillary), and Mucinous according to the WHO Classification of the Thoracic Tumors (22,23). The clinical data were collected through a review of patient records. The baseline characteristics of the study cohort are exhibited in Table S1. This study was conducted in accordance with the Declaration of Helsinki (as revised in 2013). This study was approved by the Ethics Review Committee of Peking Union Medical College Hospital (approval No. HS-3101), and written informed consent was obtained from all study participants for the use of tissue samples.

TILs quantification

As previously described, a four-tier TIL grading scheme was utilized to score the TILs on HE staining slides (24). Briefly, the score was the product of the percentage of mononuclear immune cells (including lymphocytes and plasma cells) within the tumor stroma. It was defined as following: 0 = 0–5%, 1 = 6–25%, 2 = 26–50% and 3 >50%. 0: The stroma is characterized by a completely loose or dense fibroblastic pattern with an absence or near absence of immune cells. 1: TILs are observed in a loose, scattered distribution within the stroma. 2: TILs are frequently found in proximity to neoplastic epithelial cells, and in certain areas of the stroma, they form scattered lymphocytic clusters. 3: There is a highly dense infiltration of immune cells throughout the stroma. To obtain an estimate of the mean infiltrative area, TILs were assessed in 5 stromal regions rather than in hot spots. Two experienced pathologists blinded to other clinical information carried out the quantification independently. In instances of significant disagreement between the two pathologists regarding the quantification, a third pathologist was consulted. The case was then reviewed collectively, and a discussion was held until a consensus was achieved. As for the immune status, score 3 was defined as the hot immune status, while score <3 was defined as the cold immune status. The immune scores are listed in Table S1.

TLSs quantification

TLSs quantification was performed based on HE staining and CD21 IHC staining in whole tissue slides according to the previous study (25). In the HE staining, TLS was defined as the composition of both lymphoid aggregates and follicles. TLS presented clearly visible foci of immune cells with segregated light zone and dark zone organizations. Lymphoid follicles were defined as aggregates of lymphocytes with a germinal center (mature TLS, CD21 positive TLS), while other lymphoid patterns were ignored. TLS quantification was evaluated independently by two experienced pathologists, who were blinded to other patients' information. In instances of significant disagreement between the two pathologists regarding the quantification, a third pathologist was consulted. The case was then reviewed collectively, and a discussion was held until a consensus was achieved.

IHC

Formalin-fixed, paraffin-embedded samples were collected for IHC assay. The whole slides were baked at 60 ℃ for 40 minutes to deparaffinized. Then the slides were incubated with the primary antibodies overnight at 4 ℃ in a humidified chamber. Primary antibodies used in our study were as follows: CD21 (#PA0171, Leica, Wetzlar, Germany), ALK (clone D5F3, Ventana), LAG3 (#ab209236, 1:100, Abcam, Cambridge, UK). Between each step, the slides were washed with PBS buffer twice. After mounting, the stained slides were scanned into electronic sections for further evaluation.

For the assessment of LAG-3 expression, two pathologists blinded to clinical information manually counted LAG-3$^+$ tumor-associated lymphocytes in six 400× high-power fields (0.24 mm^2 per field) and calculated the mean immune cell proportion score (IPS) as described previously (26). The LAG-3$^+$ lymphocytes were defined as expressing punctate, cytoplasmic, or membranous LAG-3. The IPS score was calculated as the percentage of LAG-3$^+$ lymphocytes in all the tumor-associated lymphocytes. Samples were classified as LAG-3 positive if the number of LAG-3$^+$ lymphocytes was ≥1% of all cells (27). In instances of significant disagreement between the two pathologists regarding the quantification, a third pathologist was consulted. The case was then reviewed collectively, and a discussion was held until a consensus was achieved.

Nucleic acid extraction and quality control assessment

Nucleic acid extraction and purification reagents (YCP-

1301 and YCP-1201, Zhenyue Biotech) were used to extract DNA and RNA from samples as per the manufacturer's instructions. The extracted nucleic acids were quantified using Qubit 4.0 (Thermo Fisher Scientific, Waltham, MA, USA), with a DNA yield of no less than 300 ng and an RNA yield of no less than 30 ng. Additionally, RNA quality was assessed using a 2100 Bioanalyzer (Agilent, location), with a DV200 (percentage of fragments >200 nucleotides) of ≥30. Sample quality control included parameters such as target reads, mapping ratio and housekeeping gene counts. If any of these parameters did not meet the criteria, the data were considered substandard.

Next-generation sequencing (NGS) for DNA and RNA

Targeted sequencing for DNA and RNA was performed using hybrid capture-based targeted NGS as previously described (28). Briefly, barcoded libraries were hybridized into a targeted panel of genes. Sequencing was conducted using the high-throughput rapid sequencing reagent kits (MGISEQ-2000 and MGISEQ-2000RS, Wuhan MGI Tech, China). Finally, bioinformatics data processing was performed by Genecast Biotechnology Co., Ltd to identify the driver mutations in the samples.

For gene variants analysis, including single-nucleotide variants (SNVs), insertions and deletions (InDel), copy number variations, and gene rearrangements, alignment analysis was performed using GATK v4.2.0 software and Vardict v1.5.1 software. The splice exon sequences of the human reference genome hg19 (GRCh37) were used as reference. Annotation of the identified mutations was carried out using the annotation modules of the ANNOVAR v0700 and TransVar v2.3.4. in HGVS format and the COSMIC database. For RNA fusion analysis, MONO v4.0.30319 in conjunction with FusionMap v8.0.2.32 and Arriba v1.2.0 were used, and the COSMIC database was used subsequently to annotate the fusion detection results.

multi-IF

Multi-IF staining was performed on whole slide sections according to the manufacturer's protocol (#AXT371000, Alpha X Bio, China). Briefly, sections were baked at 65 ℃ for 1 h, dewaxed with xylene, and rehydrated with a graded series of ethanol solutions ethanol. For epitope retrieval, slides were placed in a microwave with antigen retrieval buffer for 45 s at 100% power followed by an additional 15 min at 20% power. After blocking, the tissue sections were incubated with anti-CD3 (#ZM0417, 1:200, ZSGB-BIO, Beijing, China), anti-CD4 (#ZM0418, 1:100, ZSGB-BIO), anti-CD20 (#ab78237, 1:200, Abcam), anti-CD56 (#ZM0057, 1:100, ZSGB-BIO), anti-FOXP3 (#ab20034, 1:100, Abcam), anti-PanCK (#ZM0069, 1:300, ZSGB-BIO) respectively at 4 ℃ overnight in a staining tray. The next morning, slides were incubated with secondary antibodies and opal fluorophore working solution for 10 min at room temperature, respectively. Slides were stripped with microwave treatment until all targets of interest were detected. Subsequently, slides were incubated with DAPI working solution for 5 min at room temperature and covered with mounting medium, ready for image acquirement. The representative images from each sample were acquired with the microscope slide scanner (ZEISS AXIOSCAN 7, ZEISS, Oberkochen, Germany), and analyzed by the Halo platform (Indica Labs, Albuquerque, NM, USA). The acquired channels were as follows: CD3-520 nm/green, CD4-480 nm/cyan, CD56-570 nm/orange, FOXP3-620 nm/red, CD20-690 nm/white, PanCK-780 nm/purple, and DAPI-blue. Some parameters, including positive cell density and the rate of positive cells in the tumor compartment, were determined in the tumor compartment.

Statistical analyses

For categorical and continuous variables, Fisher's exact test and unpaired *t*-test were utilized for comparison, respectively. The two-stage linear step-up procedure of Benjamini, Krieger, and Yekutieli was utilized for the false discovery rate (FDR) approach. PFS was defined as the time from the start of surgical time or induction therapy until the progression of disease or death from any cause. The Kaplan-Meier (KM) survival curve and the log-rank test were used to analyze the significant differences. The logistic regression model and Cox proportional hazard model were used for univariate analysis and multivariate analysis. The P value was based on a two-sided hypothesis, and the P value <0.05 was considered statistically significant. All analyses were carried out with GraphPad Prism (V.8.0.1, La Jolla, CA, USA) or R software (version 4.1.3).

Results

The DNA-NGS results of the cohort are shown in Figure S1. There were 91% (62/68) of cases identified with specific ALK fusion type by DNA-NGS. Six ALK IHC-

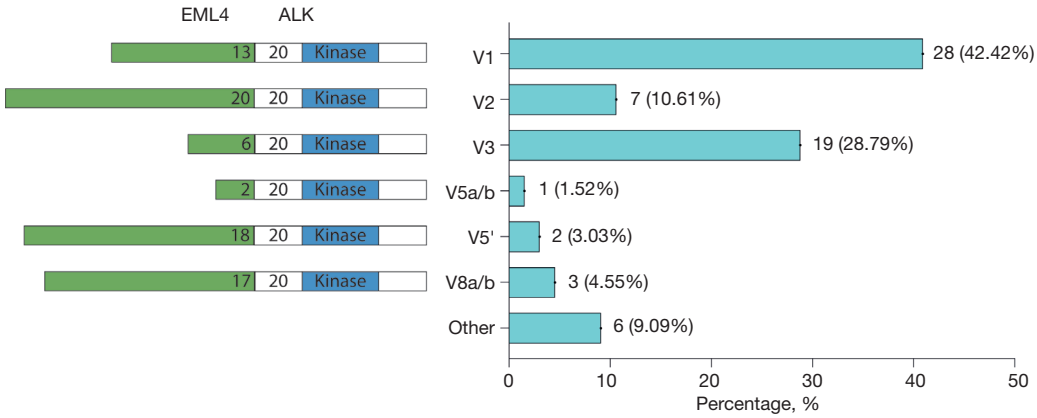

Figure 2 Distribution of different ALK fusion variants in the study cohort. EML4, Echinoderm microtubule-associated protein-like 4; ALK, anaplastic lymphoma kinase.

positive cases were identified without ALK fusion by DNA-NGS, which were further validated using RNA-NGS. Based on RNA-NGS, four of these six cases were detected with ALK fusion, including two cases with EML4-ALK V3, one case with KLC1-ALK, and one case with EML4-ALK V2. The remaining two ALK IHC-positive cases were not detected with ALK fusion by either DNA-NGS or RNA-NGS, which were excluded for further study.

In general, 66 cases with known ALK fusion variants were identified. The distributions of ALK variants in the study cohort are shown in *Figure 2*, and the details of ALK fusion variants are listed in Table S1. As expected, the most common ALK fusion variant was EML4-ALK V1 (28/66, 42.42%), following by EML4-ALK V3 (19/66, 28.79%) and EML4-ALK V2 (7/66, 10.61%). Six cases were detected with other uncommon ALK fusion variants, of which 3 were KLC1-ALK, 1 was STRN-ALK, 1 was DCTN1-ALK, and 1 was ITSN2-ALK. These 6 cases were excluded from the present study.

Comparison of clinicopathological characteristics between long-variant and short-variant groups

The EML4-ALK fusion types are illustrated in the left panel of *Figure 2*. Based on the presence of the TAPE domain of EML4 protein, cases with EML4-ALK fusion variants were divided into two subgroups, long variants (V1, V2, V5', V8 a/b) and short variants (V3 and V5 a/b). The clinical characteristics of these 60 cases are summarized in *Table 1*. Cases with short variants showed significantly larger tumor size than those with long variants (1.85±0.65 *vs.* 2.54±1.95 cm, P=0.046). According to the 8th edition of the American Joint Committee on Cancer (AJCC) staging system (29), most long-variant patients (28/40, 70.0%) had stage I–II disease, and the remaining patients (12/40, 30.0%) had stage III–IV disease. In contrast, among patients with short variants, most patients (12/20, 60.0%) were stage III–IV diseases, and 8 of 20 (40.0%) patients were at stage I–II. The AJCC stage was significantly associated with the ALK fusion variants (P=0.049). There were no significant differences in age, gender, or smoking status between these two ALK fusion variant subsets.

The pathological characteristics of these 60 cases are summarized in *Table 2*. There were no significant differences in predominant histological pattern, spread through air spaces (STAS), lymphovascular space invasion (LVI), lymph node (LN) metastasis, or distant metastasis between these two ALK variant groups.

Comparison of immune microenvironment between long-variant and short-variant groups

TILs contribute to the predominant immune cell population in the tumor immune microenvironment (30). Thus, we investigated the difference in the immune microenvironment between the long-variant and short-variant groups. Based on the assessment criteria illustrated in *Figure 3A-3D*, the cohort was classified into four semi-quantitative categories according to the TIL level (24). As shown in *Table 3* and *Figure 3E*, the TIL score was significantly associated with ALK fusion variants (P=0.02). Notably, a higher proportion of short-variant patients (70.0%, 14/20) exhibited a 'hot' immune status, characterized by a TIL score of 3, compared to long-variant patients, where only 35.0% (14/40) had a

Table 1 Clinical characteristics of EML4-ALK positive LUAD

Variables	Long variants (n=40)	Short variants (n=20)	P value
Age (mean ± SD, years)	55.58±11.63	51.35±11.09	0.18
<65	30	19	
≥65	10	1	
Gender			0.26
Male	17	5	
Female	23	15	
Smoking status			0.34
Current or ever	12	3	
Never	28	17	
Tumor size (cm)	1.85±0.65	2.54±1.95	0.046
AJCC stage			0.049
I–II	28	8	
III–IV	12	12	

EML4, echinoderm microtubule-associated protein-like 4; ALK, anaplastic lymphoma kinase; LUAD, lung adenocarcinoma; SD, standard deviation; AJCC, American Joint Committee on Cancer.

Table 2 Pathological characteristics of EML4-ALK positive LUAD

Variables	Long variants (n=40)	Short variants (n=20)	P value
Pattern			
Lepidic	0	0	>0.99
Acinar	15 (37.5%)	8 (40.0%)	
Papillary	5 (12.5%)	5 (25.0%)	
High grade	15 (37.5%)	5 (25.0%)	
Mucinous	5 (12.5%)	2 (10.0%)	
STAS	23 (57.5%)	10 (50.0%)	0.60
LVI	8 (20.0%)	3 (15.0%)	0.74
LN metastasis	12 (30.0%)	12 (60.0%)	0.055
Distant metastasis	1 (2.5%)	1 (5.0%)	>0.99

EML4, echinoderm microtubule-associated protein-like 4; ALK, anaplastic lymphoma kinase; LUAD, lung adenocarcinoma; STAS, spread through air spaces; LVI, lymphovascular space invasion; LN, lymph node.

'hot' immune status. This association between 'hot' immune status and ALK fusion variants was found to be statistically significant (P=0.01) (24). Thus, cases with short variants may be associated with a greater enrichment of immune cells within the tumor microenvironment (TME).

To compare the difference in immune cell profiles between these two groups, multi-IF was further performed. Due to limited tissue available, multi-IF was performed in 20 cases with hot immune status, including 10 cases with long variants and 10 cases with short variants. CD3, CD4, CD20, CD56, FOXP3, and panCK were used to label immune cells, that T cells ($CD3^+$), NK cells ($CD56^+$), B cells ($CD20^+$), helper T cells ($CD3^+CD4^+$), regulatory T cells ($CD3^+CD4^+FOXP3^+$), and cancer cells ($panCK^+$)

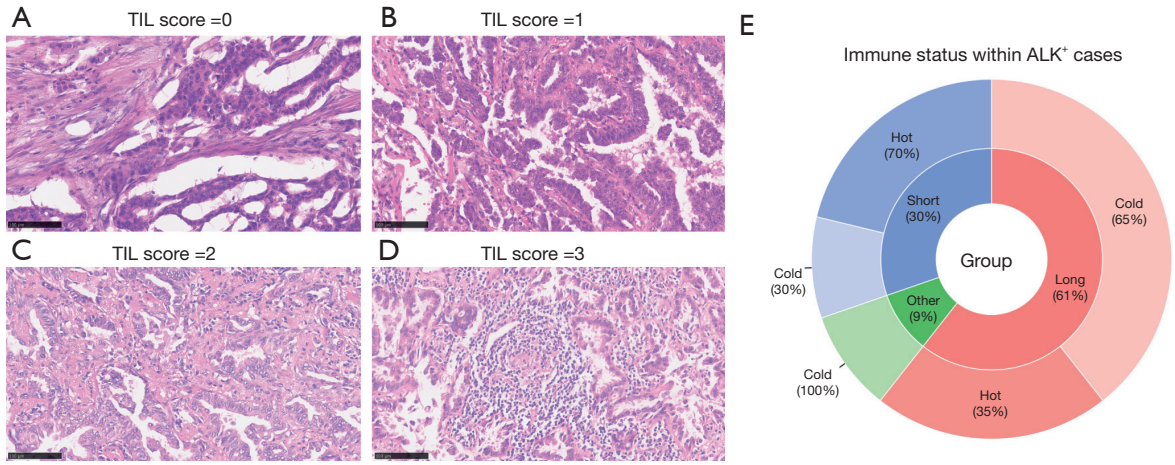

Figure 3 Short ALK fusion variants were associated with hot immune status. (A-D) Representative HE staining images for TIL score quantification (scale bar: 100 μm). (E) Distribution of immune status in patients with EML4-ALK fusion variants. EML4, echinoderm microtubule-associated protein-like 4; ALK, anaplastic lymphoma kinase; HE, hematoxylin-eosin; TIL, tumor-infiltrating lymphocyte.

Table 3 Immune characteristics of EML4-ALK positive LUAD

Variables	Long variants (n=40)	Short variants (n=20)	P value
TIL score			0.02
0	1 (2.5%)	2 (10.0%)	
1	10 (25.0%)	2 (10.0%)	
2	15 (37.5%)	2 (10.0%)	
3	14 (35.0%)	14 (70.0%)	
Immune status			0.01
Hot (score 3)	14 (35.0%)	14 (70.0%)	
Cold (score <3)	26 (65.0%)	6 (30.0%)	

EML4, echinoderm microtubule-associated protein-like 4; ALK, anaplastic lymphoma kinase; LUAD, lung adenocarcinoma; TIL, tumor-infiltrating lymphocyte.

(*Figure 4A*). As shown in *Figure 4B,4C*, both the percentage (P<0.001) and the density (P<0.001) of $CD20^+$ B cells within the stromal area in the long variants group were higher than those in the short variants group. In contrast, more $CD56^+$ NK cells, including the cell percentage (P=0.047) and cell density (P=0.03) were detected in the stromal area of the short variants group than in the long variants group. Nevertheless, there were no significant differences in total T cells, helper T cells, or Treg cells between the long variants and short variants.

TLS has been considered as a favorable prognostic factor and also promotes immune responses (31,32). Thus, the presence of TLS in the hot immune status cases was analyzed by HE staining and CD21 IHC. TLSs were defined as aggregates of lymphocytes with a germinal center (mature TLS, CD21 positive TLS), while other lymphoid patterns were ignored (*Figure 5A*). As shown in *Table 4* and *Figure 5B*, the presence of TLS was significantly associated with long variants than short variants (P=0.046). 85.7% of long ALK fusion variant cases were identified with the structure of TLS, while only 42.9% of short ALK fusion variant cases were identified with the structure of TLS. Thus, it appears that the long variants are more closely associated with the development of TLS than the short variants.

In general, the short ALK fusion variant can enrich more

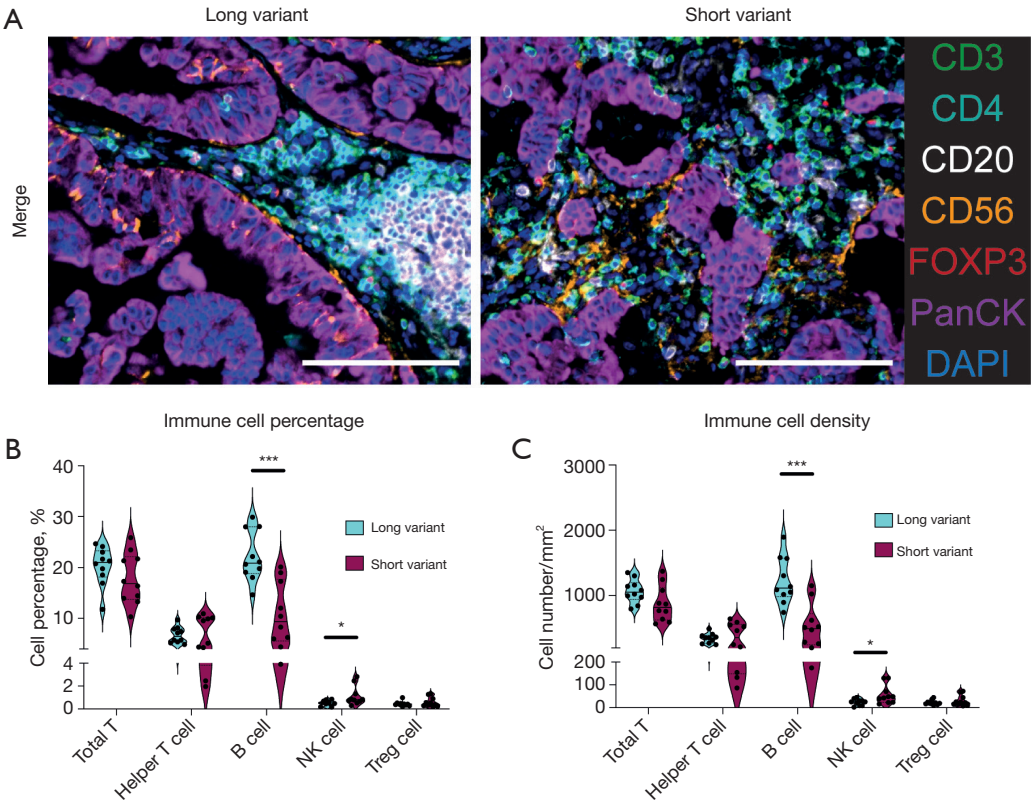

Figure 4 More NK cells enriched in patients with short ALK fusion variants. (A) Representative images for multi-fluorescence staining (scale bar: 100 μm). (B) Violin plot for immune cell percentage between long variants and short variants. (C) Violin plot for immune cell density between long variants and short variants. An unpaired *t*-test was used to compare the immune cell profile between ALK fusion variants. *, P<0.05; ***, P<0.001; ALK, anaplastic lymphoma kinase; NK, natural killer.

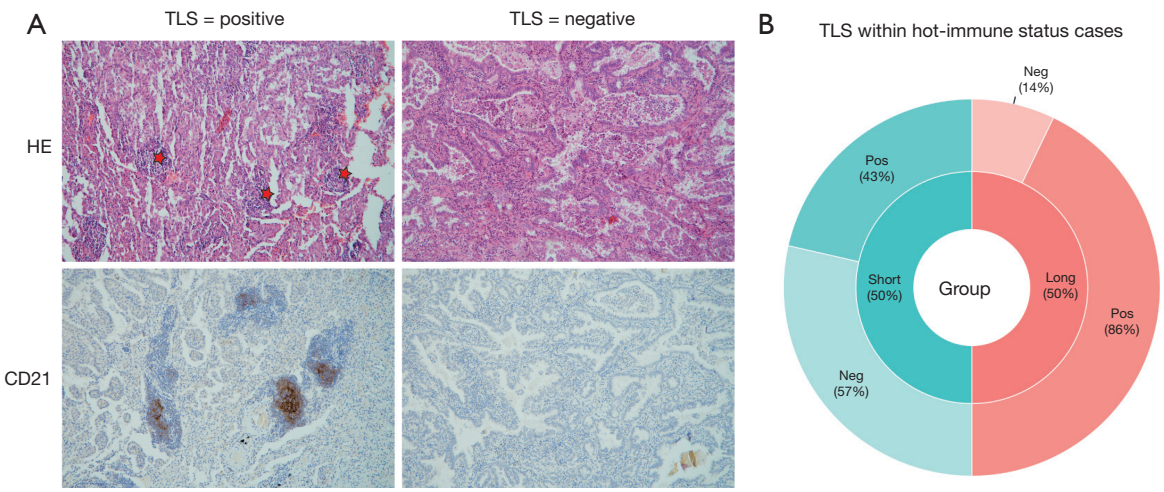

Figure 5 TLS enriched in patients with long ALK fusion variants. (A) Representative TLS images for HE staining and CD21 staining (the red star labels the TLS structure; 100×). (B) Distribution of TLS in patients with hot immune status. ALK, anaplastic lymphoma kinase; HE, hematoxylin-eosin staining; TLS, tertiary lymphoid structure.

Table 4 TLS characteristics of EML4-ALK positive LUAD

Variables	Long variants (n=14)	Short variants (n=14)	P value
Hot immune status			0.046
TLS	12 (85.7%)	6 (42.9%)	
non-TLS	2 (14.3%)	8 (57.1%)	

TLS, tertiary lymphoid structure; EML4, echinoderm microtubule-associated protein-like 4; ALK, anaplastic lymphoma kinase; LUAD, lung adenocarcinoma.

TIL but develop less TLS formation, than the long ALK fusion variant.

Prognostic impact of ALK variants and immune properties

Given that the overall survival (OS) was not reached within 60 patients censored, the PFS instead was analyzed in patients with advanced stage (III–IV stage). PFS was measured as the time from the date of surgical resection to the date of progression or censorship at the last follow-up. The median follow-up duration was 41.77 months (range from 13.80 to 61.27 months). In the univariate analysis (*Figure 6A*), only hot immune status was identified to be a negative prognostic factor [hazard ratio (HR) 8.90; 95% confidence interval (CI): 1.10 to 70.00; P=0.04]. Other characteristics, including age, gender, smoking status, short variants, positive LVI, and positive LN metastasis showed no significant correlation with the PFS. In our cohort, patients in the short ALK fusion variant tumor cohort had a significantly shorter PFS than those in the long ALK fusion variant tumor cohort (HR: 0.24, 95% CI: 0.07–0.83, P=0.050) (*Figure 6B*). Additionally, the median PFS was significantly shorter for hot immune status than that for cold immune status (HR: 8.62, 95% CI: 2.49–29.77, P=0.01) (*Figure 6C*). Moreover, ALK$^+$ LUAD patients with short ALK fusion variants with hot immune status had relatively shorter PFS than other patients, though without statistical differences (*Figure 6D*).

We further explored the impact of immune cells on the PFS in ALK$^+$ LUAD patients (*Figure* 7). In our cohort, patients with tumors exhibiting high levels of NK cell infiltration tended to have a shorter PFS than those with low levels of NK cell infiltration (HR: 4.63, 95% CI: 0.80–26.84, P=0.13) (*Figure* 7*A*). In the subgroup analysis based on the ALK fusion variant, patients with short ALK variant/high NK cells trended towards shorter PFS among subgroups as shown in *Figure* 7*D* (P=0.28). In contrast, patients with high-level intratumoral B cells had a significantly longer PFS than those with low-level intratumoral B cells (HR: 0.12, 95% CI: 0.03–0.47, P=0.02) (*Figure* 7*B*). Notably, patients with long ALK variant/high B cells showed a trend toward longer PFS compared to other subgroups as shown in *Figure* 7*E* (P=0.051). Regarding the prognosis effect of TLS, ALK$^+$ LUAD patients with positive TLS tended to have a longer PFS than those with negative TLS (HR: 0.37, 95% CI: 0.09–1.50, P=0.12) (*Figure* 7*C*). Among the subgroups based on ALK fusion variants and TLS, patients with the long ALK variant and positive TLS trended towards longer PFS, followed by those with long ALK variant and negative TLS, short ALK variant and positive TLS, and short ALK variant and negative TLS as shown in *Figure* 7*F* (P=0.054).

LAG3 expression among different ALK fusion variants

Given that short-variant patients were characterized with high TILs and NK cell infiltration, we further explored the possibility of NK cell-targeted immune therapy in ALK$^+$ LUAD patients. LAG3 has been identified as a central regulator of immune function in NK cells as well as T cells (33). Thus, anti-LAG3 drugs have been developed as a novel immune therapy, which show significant efficacy in the treatment of melanoma (27). We evaluated LAG3 expression by IHC in ALK$^+$ patients with hot immune status. IPS score was calculated as described in the method. The representative LAG3 staining image is shown in Figure S2. As shown in *Table 5*, 53.8% (7/13) of long variants expressed LAG3 with an IPS score above 1. In contrast, 76.9% (10/13) of short variants expressed LAG3 with an IPS score above 1. Moreover, two IPS scores of short-variant cases were above 10. In contrast, all IPS scores of long-variant cases were below 10. Though without statistical differences, short variants tended to enrich more LAG3$^+$ immune cells than long variants, indicating that these patients might be beneficial for anti-LAG3 immune therapy.

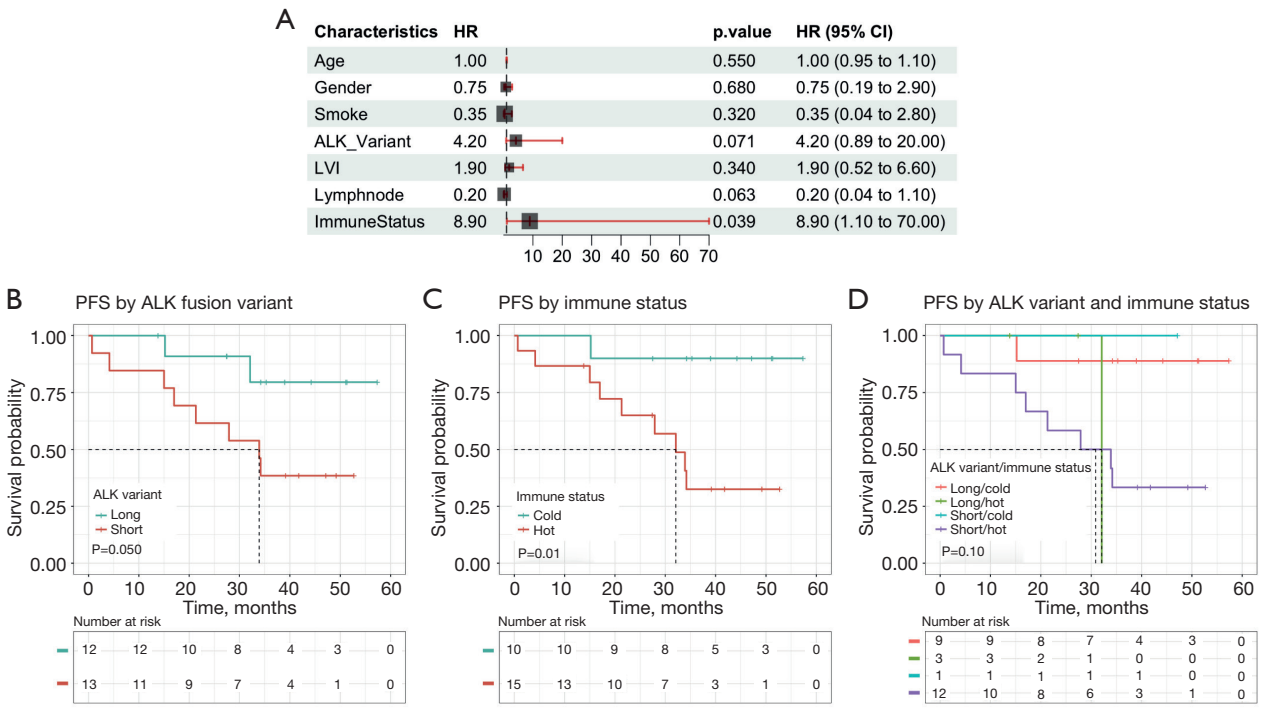

Figure 6 The impact of characteristics on the PFS of LUAD patients with EML4-ALK fusion variants in the advanced stage. (A) Univariate analysis of characteristics on the progression-free survival in patients with EML4-ALK fusion variants. (B) PFS Kaplan-Meier curve stratified by ALK fusion variants. (C) PFS Kaplan-Meier curve stratified by immune status. (D) PFS Kaplan-Meier curve stratified by ALK fusion variants and immune status. For univariate analysis, the logistic regression model and Cox proportional hazard model was used. For PFS analysis, a log-rank test was used for comparisons. P value <0.05 was considered statistically significant. PFS, progression-free survival; LUAD, lung adenocarcinoma; EML4, echinoderm microtubule-associated protein-like 4; ALK, anaplastic lymphoma kinase; HR, hazard ratio; CI, confidence interval; LVI, lymphovascular space invasion.

Discussion

To our knowledge, this is the first study to comprehensively investigate the immune microenvironment properties as well as their impacts on clinical outcomes across different ALK fusion variants. LUAD patients with short ALK fusion variant-driven tumors exhibited more aggressive behaviors with higher AJCC stage as well as larger tumor volume than those in patients with long ALK fusion variant-driven tumors. Compared to long ALK fusion variants, there were more TILs, especially NK cells, within short ALK variants. However, fewer TLS were established within short ALK variants than in long ALK variants. Furthermore, short ALK variants, hot immune status, and high-level NK cells were identified to be negative prognostic factors for clinical outcomes in LUAD patients with ALK fusion. In contrast, high-level B cells, as well as the development of TLS were identified to be positive prognostic factors for clinical outcomes in LUAD patients with ALK fusion. Finally, $LAG3^+$ immune cells were more enriched in short ALK variants than long ALK variants, indicating that anti-LAG3 therapy could be beneficial for ALK^+ LUAD patients, especially for those carrying short ALK fusion variants.

In line with previous studies (12,34), ALK^+ LUAD patients with short fusion variants exhibited a higher AJCC stage, as well as decreased PFS, than those with long fusion variants. Besides, in our present study, the short ALK fusion variant was associated with a significantly larger tumor volume and a relatively high incidence of LN metastatic. A biochemical explanation for the potentially oncogenic impact of short ALK fusion variants is of interest to be investigated. Owing to the lack of the TAPE domain, short ALK fusion protein complexes have a more stable structure as well as a longer half-life than long ALK fusion protein complexes, resulting in stronger oncogenic signaling activation *in vitro* (11). In addition, O'Regan

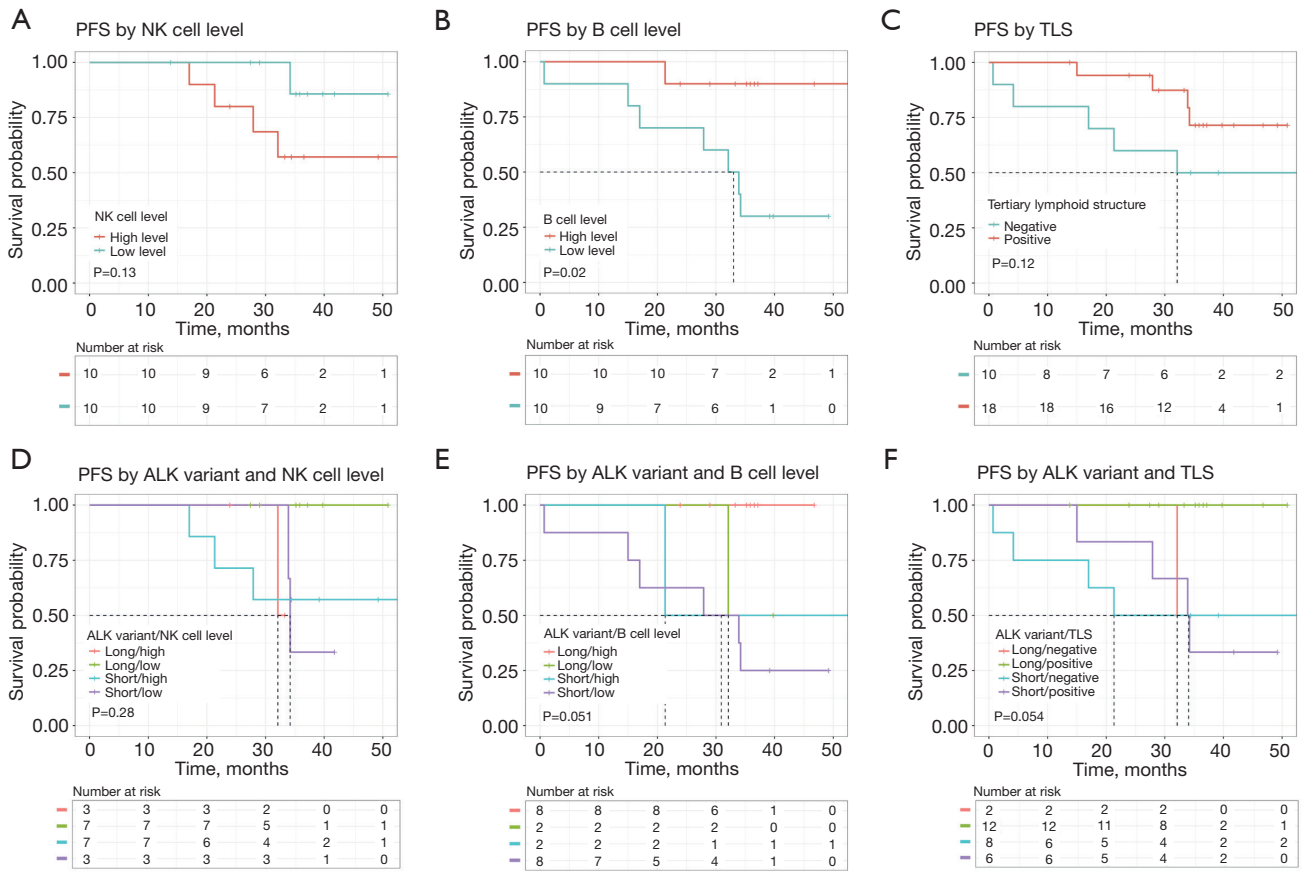

Figure 7 The impact of immune characteristics on the PFS of LUAD patients with EML4-ALK fusion variants. (A) PFS Kaplan-Meier curve stratified by NK cell level. (B) PFS Kaplan-Meier curve stratified by B cell level. (C) PFS Kaplan-Meier curve stratified by TLS structure. (D) PFS Kaplan-Meier curve stratified by ALK fusion variants and NK cell level. (E) PFS Kaplan-Meier curve stratified by ALK fusion variants and B cell level. (F) PFS Kaplan-Meier curve stratified by ALK fusion variants and TLS. For PFS analysis, a log-rank test was used for comparisons. P value <0.05 was considered statistically significant. PFS, progression-free survival; LUAD, lung adenocarcinoma; EML4, echinoderm microtubule-associated protein-like 4; NK, natural killer; TLS, tertiary lymphoid structure; ALK, anaplastic lymphoma kinase.

Table 5 LAG3 expression in EML4-ALK positive LUAD with hot immune status

LAG3 (IPS score)	Long variants (n=13)	Short variants (n=13)	P value
<10 *vs.* ≥10			0.48
<10	13 (100.0%)	11 (84.6%)	
≥10	0	2 (15.4%)	
<1 *vs.* ≥1			0.41
<1	6 (46.2%)	3 (23.1%)	
≥1	7 (53.8%)	10 (76.9%)	

EML4, echinoderm microtubule-associated protein-like 4; ALK, anaplastic lymphoma kinase; LUAD, lung adenocarcinoma; LAG3, lymphocyte-activation gene-3; IPS, immune cell proportion score.

et al. have discovered that EML4-ALK V3, rather than EML4-ALK V1, can localize to spindle microtubule and induce cell migration via activation of NEK kinase family NEC7/NEC9 (35). Such binding can contribute to cellular migration and thus promote metastatic spread, which explains the relatively high incidence of LN metastatic in patients with short variants. Herein, the combination of microtubule inhibitors along with TKI treatment can lead to a synergistic response in the short ALK fusion variant and thus overcome the TKI resistance caused by the short ALK fusion variant (36). Collectively, combined with our results and previous results, the short ALK fusion variants should serve as a risk factor in ALK$^+$ LUAD, conferring an aggressive behavior, which requires more effective therapeutic strategies beyond TKIs.

To date, no research has been performed to characterize the immune cell infiltration among different ALK fusion variants. Yang *et al.* have performed multi-IF to profile the immune cells in three ALK$^+$ cases, including one case with EML4-ALK V1 and one case with EML4-ALK V3 (20). They have found that compared to the V1 case, the V3 case enriched a smaller extent of immune cell infiltration. However, their limited samples can result in sampling bias, making it difficult to achieve a meaningful conclusion. Contrary to this, our study found that most cases with short ALK fusion variants exhibited robust immune cell infiltration, especially CD56$^+$ NK cell infiltration. Interestingly, these cases with hot immune status had worse outcomes than other patients, which is against the common point that the high proportion of TILs as well as CD56$^+$ NK cell infiltration, is correlated with a favorable prognosis in LUAD (37-39). A possible explanation for this might be that most enriched TILs within the short ALK fusion variants have been remodeled to be immune-impaired and exhausted (40). The exhausted TILs can facilitate the immune escape of tumor cells and thus support tumor progression (41). In our study and previous studies, less TLS formation and more exhausted immune marker expression, such as LAG3 and PD-L1, were observed in patients with short variants than in those with long variants (20). In the meanwhile, Chuang *et al.* have found that cancer cells harboring EML4-ALK V3, rather than EML4-ALK V1, can inhibit NK cell-mediated cytotoxicity by secreting immunosuppressive molecules (19). All these results suggest that the interface between ALK fusion cancer cells and immune cells does exist, and the impacts of cancer cells on immune cells are heterogeneous among different ALK fusion variants. The immune cells within the microenvironment from short ALK fusion variants could be less active and skewed towards relative suppression than other ALK fusion variants. However, more work is needed to shed light on such speculation, which can improve our understanding of the immune remodeling within ALK$^+$ cancers, and further development of novel therapeutic targets for ALK$^+$ LUAD treatment.

Our study demonstrated that long variants were characterized with more TLS as well as better prognosis than short variants. These data corroborate the notion that the presence of TLS serves as a favorable predictor of LUAD survival (31,42). It should be noted that TLS can be classified into two groups, immature TLS and mature TLS. Mature TLS, other than immature TLS, is characterized by B cell-containing germinal centers, which can expand tumor-targeting CD4$^+$ T cells as well as CD8$^+$ T cells, and thus support antitumor immune responses (43-47). In accordance with these, ALK$^+$ LUAD with long variants contained more B cell-constituting mature TLS organizations than those with short variants, which may activate the locally developed adaptive immune response and as a result, promote prognosis benefit. However, direct evidence to support this postulation is lacking, which deserves to be investigated in future studies. Moreover, the molecular mechanisms by which the cancer cells with different ALK fusion variants remodel the intertumoral immune cells and how they drive TLS organization are still unknown, which will likely emerge as a future research question.

Another key observation in our study is that most cancers with short variants had a slightly higher rate of LAG3$^+$ immune cells as compared with the long variant cohort, though without statistical significance. The negative statistical significance was likely due to the low number of tissues available for LAG3 staining in our study. However, these observations hinted that blocking LAG3 may have a remarkable anti-tumor effect in ALK$^+$ LUAD, especially for those with short variants. Beyond the common PD-1/PD-L1 therapy, which has been demonstrated inefficiency in ALK$^+$ LUAD treatment (48,49), anti-LAG3 therapy holds promise to be an alternative or synergistic therapy for TKI-based regimens. LAG3 has been identified as the main controller receptor of NK cells, to orchestra immune functions of NK cells (33). Blockade of LAG3 by antibodies can enhance cytokine production to activate cytotoxicity function in NK cells. Combined with our finding that the short variant can enrich more NK cells, anti-LAG3 therapy is theoretically effective for ALK$^+$ LUAD patients

with short variants, even though the real-world data is limited. Recently, the clinical trial NEOpredict-Lung (NCT04205552) has demonstrated the feasibility and safety of preoperative dual targeting of PD-1 and LAG-3 in patients with resectable LUAD (50). In parallel, several clinical trials using LAG-3-targeting therapies for LUAD treatment are ongoing, such as NCT03625323 and NCT01968109. These landmark trials greatly pave the way to exploring the efficacy of anti-LAG3 therapy for LUAD treatment. Collectively, our study provides a piece of premature evidence for LAG3-targeting therapy in ALK$^+$ LUAD patients, especially for ALK$^+$ LUAD patients with short variants, which is warranted for further exploration.

Limitations of the present study include those inherent to any retrospective study. First, this is a single-center, retrospective study with a small sample size, although the largest one to date. Other multicenter studies with larger patient cohorts may address these limitations. Secondly, the follow-up period in this study is relatively short, with a median of PFS 41.77 months (range from 13.80 to 61.27 months). Long-term data are more meaningful to clarify the impact of immune characteristics on the prognosis. Further results from this ALK$^+$-patient cohort are awaited. Thirdly, we only profiled immune cells specifically in the ALK$^+$ LUAD cases that exhibit a 'hot' immune status, rather than analyzing the entire tissue. It should be noted that the TME is complex, varying between 'hot' and 'cold' states. Therefore, it would be valuable to compare the immune profiles between these two distinct immunological contexts. Fourthly, we did not evaluate the signature of other types of immune cells, such as macrophages and dendritic cells. Advanced techniques like single-cell and spatial sequencing could offer valuable insights for characterizing these cells. A detailed landscape of immune cell subsets is of interest to be illustrated, which can improve our understanding of local and systemic tumor/immune cell interactions and help us optimize immune therapy selection for use in clinical practice. Last but not least, only LAG3 expression was evaluated in our study. Other novel immune therapy targets, such as TIGHT, KIR, and VISTA, deserve to be further analyzed, which can provide more options for ALK$^+$ LUAD treatment.

Conclusions

In conclusion, our study demonstrated that the tumor immune microenvironments were heterogeneous across different ALK fusion variants. We discovered that compared to long variants, ALK$^+$ LUAD with short variants were characterized by higher levels of TILs and NK cells, but less TLS development, which disfavoured disease prognosis. Considering the enrichment of LAG3$^+$ TILs, immunotherapy, such as anti-LAG-3 target therapy, could bring new therapeutic possibilities for ALK-rearranged patients with short variants, which requires further exploration and validation by clinical trials.

Acknowledgments

Funding: This study was supported by National High-Level Hospital Clinical Research Funding (2022-PUMCH-A-078).

Footnote

Reporting Checklist: The authors have completed the REMARK reporting checklist. Available at https://tlcr.amegroups.com/article/view/10.21037/tlcr-24-682/rc

Data Sharing Statement: Available at https://tlcr.amegroups.com/article/view/10.21037/tlcr-24-682/dss

Peer Review File: Available at https://tlcr.amegroups.com/article/view/10.21037/tlcr-24-682/prf

Conflicts of Interest: All authors have completed the ICMJE uniform disclosure form (available at https://tlcr.amegroups.com/article/view/10.21037/tlcr-24-682/coif). The authors have no conflicts of interest to declare.

Ethical Statement: The authors are accountable for all aspects of the work in ensuring that questions related to the accuracy or integrity of any part of the work are appropriately investigated and resolved. This study was reviewed and approved by the Ethics Review Committee of Peking Union Medical College Hospital (approval No. HS-3101). The study was conducted in accordance with the Declaration of Helsinki (as revised in 2013). Informed consent was obtained from all study participants to use tissue samples.

References

1. Du X, Shao Y, Qin HF, et al. ALK-rearrangement in non-small-cell lung cancer (NSCLC). Thorac Cancer 2018;9:423-30.
2. Shaw AT, Bauer TM, de Marinis F, et al. First-Line Lorlatinib or Crizotinib in Advanced ALK-Positive Lung Cancer. N Engl J Med 2020;383:2018-29.
3. Peters S, Camidge DR, Shaw AT, et al. Alectinib versus Crizotinib in Untreated ALK-Positive Non-Small-Cell Lung Cancer. N Engl J Med 2017;377:829-38.
4. Shaw AT, Kim TM, Crinò L, et al. Ceritinib versus chemotherapy in patients with ALK-rearranged non-small-cell lung cancer previously given chemotherapy and crizotinib (ASCEND-5): a randomised, controlled, open-label, phase 3 trial. Lancet Oncol 2017;18:874-86.
5. Camidge DR, Kim HR, Ahn MJ, et al. Brigatinib versus Crizotinib in ALK-Positive Non-Small-Cell Lung Cancer. N Engl J Med 2018;379:2027-39.
6. Mok T, Camidge DR, Gadgeel SM, et al. Updated overall survival and final progression-free survival data for patients with treatment-naive advanced ALK-positive non-small-cell lung cancer in the ALEX study. Ann Oncol 2020;31:1056-64.
7. Bayliss R, Choi J, Fennell DA, et al. Molecular mechanisms that underpin EML4-ALK driven cancers and their response to targeted drugs. Cell Mol Life Sci 2016;73:1209-24.
8. Mota I, Patrucco E, Mastini C, et al. ALK peptide vaccination restores the immunogenicity of ALK-rearranged non-small cell lung cancer. Nat Cancer 2023;4:1016-35.
9. Zhou X, Shou J, Sheng J, et al. Molecular and clinical analysis of Chinese patients with anaplastic lymphoma kinase (ALK)-rearranged non-small cell lung cancer. Cancer Sci 2019;110:3382-90.
10. Richards MW, Law EW, Rennalls LP, et al. Crystal structure of EML1 reveals the basis for Hsp90 dependence of oncogenic EML4-ALK by disruption of an atypical β-propeller domain. Proc Natl Acad Sci U S A 2014;111:5195-200.
11. Woo CG, Seo S, Kim SW, et al. Differential protein stability and clinical responses of EML4-ALK fusion variants to various ALK inhibitors in advanced ALK-rearranged non-small cell lung cancer. Ann Oncol 2017;28:791-7.
12. Christopoulos P, Endris V, Bozorgmehr F, et al. EML4-ALK fusion variant V3 is a high-risk feature conferring accelerated metastatic spread, early treatment failure and worse overall survival in ALK(+) non-small cell lung cancer. Int J Cancer 2018;142:2589-98.
13. Li M, Hou X, Chen J, et al. ALK fusion variant 3a/b, concomitant mutations, and high PD-L1 expression were associated with unfavorable clinical response to second-generation ALK TKIs in patients with advanced ALK-rearranged non-small cell lung cancer (GASTO 1061). Lung Cancer 2022;165:54-62.
14. Cha YJ, Kim HR, Shim HS. Clinical outcomes in ALK-rearranged lung adenocarcinomas according to ALK fusion variants. J Transl Med 2016;14:296.
15. Ettinger DS, Wood DE, Aisner DL, et al. Non-Small Cell Lung Cancer, Version 3.2022, NCCN Clinical Practice Guidelines in Oncology. J Natl Compr Canc Netw 2022;20:497-530.
16. Gainor JF, Shaw AT, Sequist LV, et al. EGFR Mutations and ALK Rearrangements Are Associated with Low Response Rates to PD-1 Pathway Blockade in Non-Small Cell Lung Cancer: A Retrospective Analysis. Clin Cancer Res 2016;22:4585-93.
17. Jahanzeb M, Lin HM, Pan X, et al. Immunotherapy Treatment Patterns and Outcomes Among ALK-Positive Patients With Non-Small-Cell Lung Cancer. Clin Lung Cancer 2021;22:49-57.
18. Shankar B, Zhang J, Naqash AR, et al. Multisystem Immune-Related Adverse Events Associated With Immune Checkpoint Inhibitors for Treatment of Non-Small Cell Lung Cancer. JAMA Oncol 2020;6:1952-6.
19. Chuang TP, Lai WY, Gabre JL, et al. ALK fusion NSCLC oncogenes promote survival and inhibit NK cell responses via SERPINB4 expression. Proc Natl Acad Sci U S A 2023;120:e2216479120.
20. Yang CY, Liao WY, Ho CC, et al. Association of Programmed Death-Ligand 1 Expression with Fusion Variants and Clinical Outcomes in Patients with Anaplastic Lymphoma Kinase-Positive Lung Adenocarcinoma Receiving Crizotinib. Oncologist 2020;25:702-11.
21. Nicholson AG, Tsao MS, Beasley MB, et al. The 2021 WHO Classification of Lung Tumors: Impact of Advances Since 2015. J Thorac Oncol 2022;17:362-87.
22. Tsao MS, Nicholson AG, Maleszewski JJ, et al. Introduction to 2021 WHO Classification of Thoracic Tumors. J Thorac Oncol 2022;17:e1-4.

23. Moreira AL, Ocampo PSS, Xia Y, et al. A Grading System for Invasive Pulmonary Adenocarcinoma: A Proposal From the International Association for the Study of Lung Cancer Pathology Committee. J Thorac Oncol 2020;15:1599-610.
24. Rakaee M, Kilvaer TK, Dalen SM, et al. Evaluation of tumor-infiltrating lymphocytes using routine H&E slides predicts patient survival in resected non-small cell lung cancer. Hum Pathol 2018;79:188-198.
25. Rakaee M, Kilvaer TK, Jamaly S, et al. Tertiary lymphoid structure score: a promising approach to refine the TNM staging in resected non-small cell lung cancer. Br J Cancer 2021;124:1680-9.
26. Shepherd DJ, Tabb ES, Kunitoki K, et al. Lymphocyte-activation gene 3 in non-small-cell lung carcinomas: correlations with clinicopathologic features and prognostic significance. Mod Pathol 2022;35:615-24.
27. Gide TN, Paver EC, Yaseen Z, et al. Lag-3 expression and clinical outcomes in metastatic melanoma patients treated with combination anti-lag-3 + anti-PD-1-based immunotherapies. Oncoimmunology 2023;12:2261248.
28. Liu Y, Wu S, Shi X, et al. ALK detection in lung cancer: identification of atypical and cryptic ALK rearrangements using an optimal algorithm. J Cancer Res Clin Oncol 2020;146:1307-20.
29. Abdel-Rahman O. Validation of the prognostic value of new sub-stages within the AJCC 8th edition of non-small cell lung cancer. Clin Transl Oncol 2017;19:1414-20.
30. Brummel K, Eerkens AL, de Bruyn M, et al. Tumour-infiltrating lymphocytes: from prognosis to treatment selection. Br J Cancer 2023;128:451-8.
31. Tamiya Y, Nakai T, Suzuki A, et al. The impact of tertiary lymphoid structures on clinicopathological, genetic and gene expression characteristics in lung adenocarcinoma. Lung Cancer 2022;174:125-32.
32. Helmink BA, Reddy SM, Gao J, et al. B cells and tertiary lymphoid structures promote immunotherapy response. Nature 2020;577:549-55.
33. Narayanan S, Ahl PJ, Bijin VA, et al. LAG3 is a Central Regulator of NK Cell Cytokine Production. bioRxiv 2020. doi: 10.1101/2020.01.31.928200.
34. Chang GC, Yang TY, Chen KC, et al. ALK variants, PD-L1 expression, and their association with outcomes in ALK-positive NSCLC patients. Sci Rep 2020;10:21063.
35. O'Regan L, Barone G, Adib R, et al. EML4-ALK V3 oncogenic fusion proteins promote microtubule stabilization and accelerated migration through NEK9 and NEK7. J Cell Sci 2020;133:jcs241505.
36. Lucken K, O'Regan L, Choi J, et al. EML4-ALK Variant 3 Promotes Mitotic Errors and Spindle Assembly Checkpoint Deficiency Leading to Increased Microtubule Poison Sensitivity. Mol Cancer Res 2022;20:854-66.
37. Takanami I, Takeuchi K, Giga M. The prognostic value of natural killer cell infiltration in resected pulmonary adenocarcinoma. J Thorac Cardiovasc Surg 2001;121:1058-63.
38. Platonova S, Cherfils-Vicini J, Damotte D, et al. Profound coordinated alterations of intratumoral NK cell phenotype and function in lung carcinoma. Cancer Res 2011;71:5412-22.
39. Brambilla E, Le Teuff G, Marguet S, et al. Prognostic Effect of Tumor Lymphocytic Infiltration in Resectable Non-Small-Cell Lung Cancer. J Clin Oncol 2016;34:1223-30.
40. Zeng Y, Lv X, Du J. Natural killer cell-based immunotherapy for lung cancer: Challenges and perspectives (Review). Oncol Rep 2021;46:232.
41. Aktar N, Yueting C, Abbas M, et al. Understanding of Immune Escape Mechanisms and Advances in Cancer Immunotherapy. J Oncol 2022;2022:8901326.
42. Xiaoxu D, Min X, Chengcheng C. Immature central tumor tertiary lymphoid structures are associated with better prognosis in non-small cell lung cancer. BMC Pulm Med 2024;24:155.
43. Schumacher TN, Thommen DS. Tertiary lymphoid structures in cancer. Science 2022;375:eabf9419.
44. Fridman WH, Sibéril S, Pupier G, et al. Activation of B cells in Tertiary Lymphoid Structures in cancer: Anti-tumor or anti-self? Semin Immunol 2023;65:101703.
45. Goc J, Germain C, Vo-Bourgais TK, et al. Dendritic cells in tumor-associated tertiary lymphoid structures signal a Th1 cytotoxic immune contexture and license the positive prognostic value of infiltrating CD8+ T cells. Cancer Res 2014;74:705-15.
46. Zeng DQ, Yu YF, Ou QY, et al. Prognostic and predictive value of tumor-infiltrating lymphocytes for clinical therapeutic research in patients with non-small cell lung cancer. Oncotarget 2016;7:13765-81.
47. Zhu W, Germain C, Liu Z, et al. A high density of tertiary lymphoid structure B cells in lung tumors is associated with increased CD4(+) T cell receptor repertoire clonality. Oncoimmunology 2015;4:e1051922.
48. Garassino MC, Cho BC, Kim JH, et al. Durvalumab as third-line or later treatment for advanced non-small-cell lung cancer (ATLANTIC): an open-label, single-arm, phase 2 study. Lancet Oncol 2018;19:521-36.
49. Solomon BJ, Mok T, Kim DW, et al. First-line crizotinib

versus chemotherapy in ALK-positive lung cancer. N Engl J Med 2014;371:2167-77.
50. Schuler M, Cuppens K, Plönes T, et al. Neoadjuvant nivolumab with or without relatlimab in resectable non-small-cell lung cancer: a randomized phase 2 trial. Nat Med 2024;30:1602-11.

Cite this article as: Xiao Y, Wang H, Lu J, Pang J, Liu S, Zhou Y, Shi X, Liang Z. Characteristics of the immune microenvironment and their clinical significance in lung adenocarcinoma patients with different ALK fusion variants. Transl Lung Cancer Res 2024;13(12):3538-3554. doi: 10.21037/tlcr-24-682